PHILOSOPHICAL TRANSACTIONS OF THE ROYAL SOCIETY A

Phil. Trans. R. Soc. A (2009) **367**, 3227–3238
doi:10.1098/rsta.2009.0073

Transition from pulses to fronts in the cubic–quintic complex Ginzburg–Landau equation

By Pablo Gutiérrez[1,2,*], Daniel Escaff[1] and Orazio Descalzi[1]

[1]*Complex Systems Group, Facultad de Ingeniería, Universidad de los Andes, Avenue San Carlos de Apoquindo 2200, Santiago, Chile*
[2]*Departamento de Física, FCFM, Universidad de Chile, Casilla 487-3, Santiago, Chile*

The cubic–quintic complex Ginzburg–Landau is the amplitude equation for systems in the vicinity of an oscillatory sub-critical bifurcation (Andronov–Hopf), and it shows different localized structures. For pulse-type localized structures, we review an approximation scheme that enables us to compute some properties of the structures, like their existence range. From that scheme, we obtain conditions for the existence of pulses in the upper limit of a control parameter. When we study the width of pulses in that limit, the analytical expression shows that it is related to the transition between pulses and fronts. This fact is consistent with numerical simulations.

Keywords: Ginzburg–Landau equation; bifurcations; localized structures

1. Introduction

In this work, we are interested in systems out of thermodynamic equilibrium, which are extended in space. This is the case for many topics in modern science, such as hydrodynamics, chemical reactions, population dynamics, nonlinear optics and granular media. One experimental example, closely related to our work, is a binary-fluid layer that is heated from below and presents localized pulses (Kolodner *et al.* 1988; Kolodner 1991).

More specifically, we are interested in bifurcations. Given a system with particular symmetries, the bifurcation sets the partial differential equations that must be used as a model. In our case, we are concerned with an oscillatory sub-critical bifurcation (Andronov–Hopf) that is modelled by the cubic–quintic complex Ginzburg–Landau (CGL) equation (van Saarloos & Hohenberg 1990, 1992; Descalzi *et al.* 2001). In this model equation, we will be interested in bifurcations between its different stable solutions.

The cubic–quintic CGL equation has demonstrated an extraordinary richness of stable solutions. Many different stable localized structures such as pulses (Thual & Fauve 1988; Deissler & Brand 1994; Afanasjev *et al.* 1996) and holes

*Author for correspondence (pagutier@gmail.com).

One contribution of 14 to a Theme Issue ‘Topics on non-equilibrium statistical mechanics and nonlinear physics’.

(Sakaguchi 1991; Descalzi & Brand 2005; Descalzi *et al.* 2005) have been observed, as well as coexistence between those structures (Hayase *et al.* 2004; Descalzi *et al.* 2006*a*) and their interactions (Descalzi *et al.* 2006*b*, 2007). However, this paper will focus only on the particular case of pulses.

From the pioneering results of Thual & Fauve (1988), many theoretical and numerical studies of pulses have been carried out (Fauve & Thual 1990; Malomed & Nepomnyashchy 1990; Hakim & Pomeau 1991). We can remark on the contribution of van Saarloos & Hohenberg (1990): they established that there is a well-defined range of parameters where pulses can be found, and also, out of that range, the system shows fronts.

Years later, Descalzi *et al.* (2002, 2003) pointed out that the emergence of pulses takes place via a saddle-node bifurcation at the lower value of a control parameter (Descalzi 2003). This important result comes from an approximation method for pulses (called a *matching approach*), which is the basis for this work too.

Recently, mathematical conditions for the transition between pulses and fronts (at the upper value of the control parameter) were obtained in order to understand the second limit of the existence range of pulses (Gutiérrez & Descalzi 2007). But at that time, the meaning of those conditions remained unclear. Our purpose now is to give an interpretation of those mathematical conditions and to make comparisons among them and numerical simulations.

2. Approximating stable localized pulses

Our starting point is the cubic–quintic CGL equation,

$$\partial_t A = \mu A + \beta |A|^2 A + \gamma |A|^4 A + D\,\partial_{xx} A, \tag{2.1}$$

where the subscripts x and t denote partial derivatives with respect to space and time, respectively. $A(x,t) = r(x,t)\exp\{i\phi(x,t)\}$ is a complex field. The control parameter μ is considered as real without losing generality. The parameters $\beta = \beta_r + i\beta_i$, $\gamma = \gamma_r + i\gamma_i$ and $D = D_r + iD_i$ are in general complex and contain the information of the physical problem under study. In order to ensure that the bifurcation is sub-critical and saturates to quintic order, it is necessary to restrict ourselves to $\beta_r > 0$ and $\gamma_r < 0$. For the homogeneous case, the system shows coexistence of stable solutions in the range $\beta_r^2/4\gamma_r \leq \mu \leq 0$.

If the localized structure is stationary, which means r is a function depending only on the space, then it is possible to make the following ansatz (Thual & Fauve 1988),

$$A(x,t) = R_0(x)\exp\{i(\Omega t + \theta_0(x))\}, \tag{2.2}$$

where Ω is an unknown parameter. Replacing the ansatz in equation (2.1) one obtains two real equations, and, after simple algebra, the results

$$0 = \mu_+ R_0 + \beta_+ R_0^3 + \gamma_+ R_0^5 + R_{0xx} - R_0\theta_{0x}^2, \tag{2.3}$$

$$\mu_- R_0 = \beta_- R_0^3 + \gamma_- R_0^5 + 2R_{0x}\theta_{0x} + R_0\theta_{0xx}, \tag{2.4}$$

with

$$\mu_+ = \frac{D_r\mu - D_i\Omega}{|D|^2}, \qquad \beta_+ = \frac{D_r\beta_r + D_i\beta_i}{|D|^2}, \qquad \gamma_+ = \frac{D_r\gamma_r + D_i\gamma_i}{|D|^2},$$

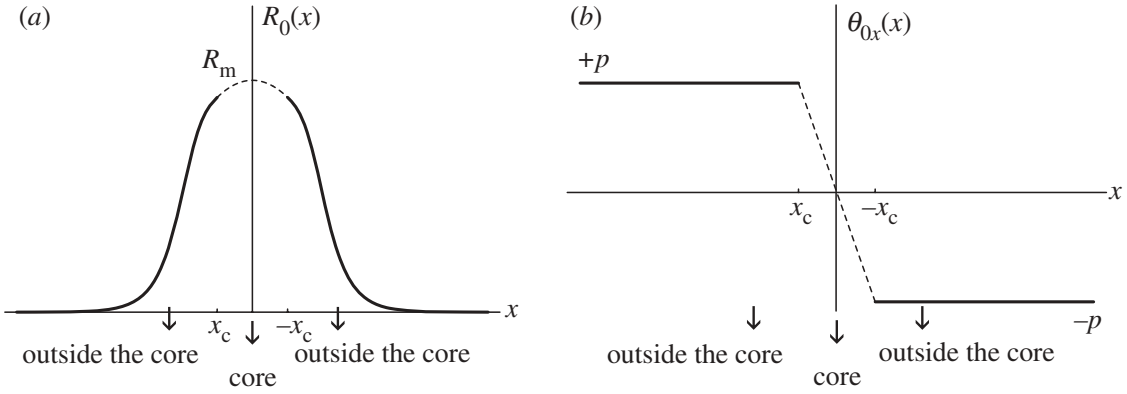

Figure 1. Regions of approximation for a pulse. The thick line is the *outside the core* region. The dotted line is the *core* region. (*a*) Modulus of the pulse R_0. (*b*) Phase gradient θ_{0x}.

$$\mu_- = \frac{D_i\mu + D_r\Omega}{|D|^2}, \qquad \beta_- = \frac{D_r\beta_i - D_i\beta_r}{|D|^2}, \qquad \gamma_- = \frac{D_r\gamma_i - D_i\gamma_r}{|D|^2}$$

and $|D|^2 = D_r^2 + D_i^2$. It is important to note that, if θ_{0x} is constant, one can explicitly integrate equation (2.3). If the associated numerical simulations are observed (Descalzi & Brand 2005; Descalzi *et al.* 2005), the validity of the condition on θ_{0x} becomes clear in almost the whole space, except around the centre of the localized structure. This numerical fact allowed Descalzi *et al.* (2002, 2003) to propose the following approximation scheme (or matching approach): the space is divided in one region near the centre of the pulse (core) and in another region out of the centre of the pulse (outside the core) (figure 1).

Outside the core, where θ_{0x} is constant ($+p$ for $x < x_c$ and $-p$ for $x > x_c$), one can explicitly integrate equation (2.3). The solution is

$$R_0(x) = \rho(|x|), \tag{2.5}$$

where

$$\rho(x) = \frac{2b^{1/4}\exp\{\sqrt{p^2-\mu_+}(x+x_0)\}}{\sqrt{(\exp\{2\sqrt{p^2-\mu_+}(x+x_0)\} + a/\sqrt{b})^2 - 4}}, \tag{2.6}$$

and $a = -3\beta_+/2\gamma_+$, $b = -3(-\mu_+ + p^2)/\gamma_+$. x_0 is a constant that emerges from the translation symmetry of the cubic–quintic CGL equation.

The frequency Ω can be asymptotically evaluated: $\Omega = (-D_i(\mu D_r - 2p^2|D|^2) + 2p|D|^2\sqrt{-\mu D_r + p^2|D|^2})/D_r^2$, which depends only on p (and on the parameters of equation (2.1)).

Inside the core, one can approximate the functions $R_0(x)$ and $\theta_{0x}(x)$ by their first terms in Taylor expansion writing

$$R_0(x) = R_m - \varepsilon x^2, \qquad \theta_{0x}(x) = -\alpha x, \tag{2.7}$$

where $(R_m, \varepsilon, \alpha)$ are unknown parameters. R_m is the maximum height of the pulse at $x = 0$.

When equations (2.7) are included in equations (2.3) and (2.4), $\varepsilon = (\mu_+ R_m + \beta_+ R_m^3 + \gamma_+ R_m^5)/2$ and $\alpha = \beta_- R_m^2 + \gamma_- R_m^4 - \mu_-$ are obtained. Now ε and α are expressed in terms of (R_m, p) and on the original parameters of equation (2.1).

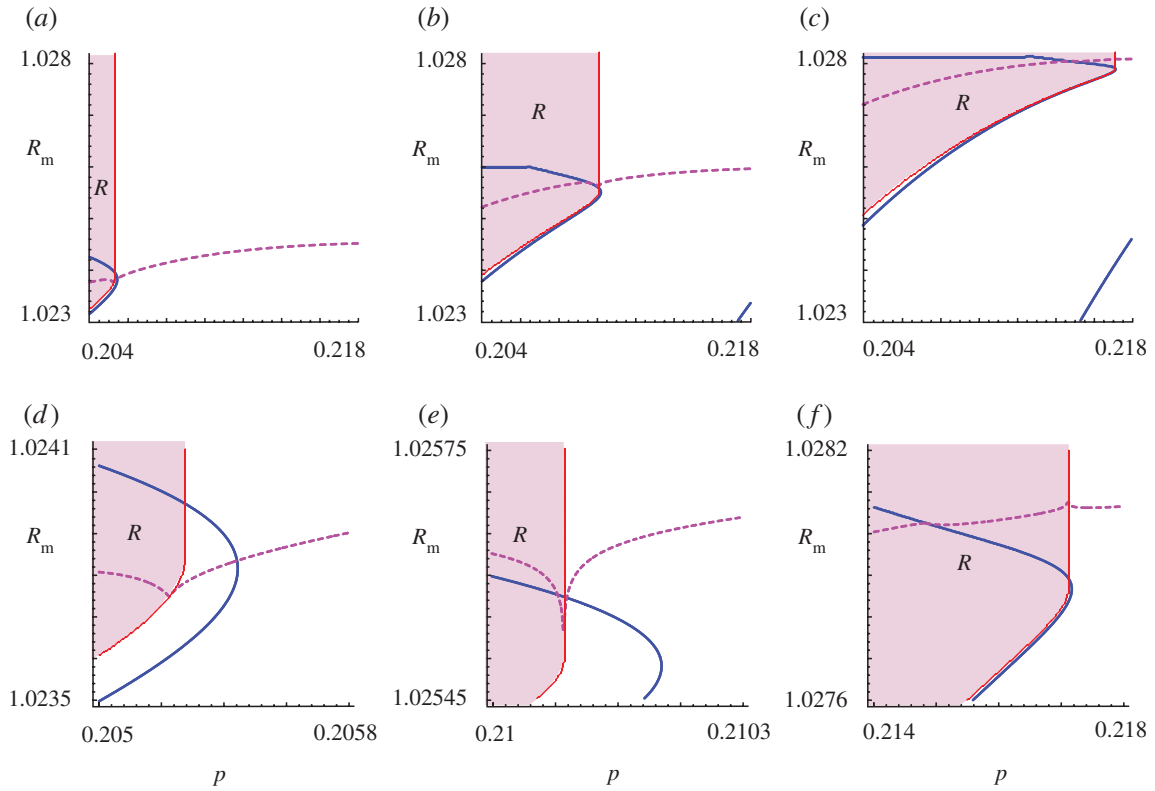

Figure 2. The (R_m, p) diagram for different μ. The blue continuous line corresponds to $f=0$. The purple dotted line corresponds to $g=0$. The region where R_0 does not exist as a real variable (which we call R) is drawn in pink and is enclosed by the thin red line. If the intersection of the blue and purple lines takes place outside R, the pulse exists ((*a*) and (*b*)). On the other hand, if the intersection takes place inside R, the pulse does not exist (*c*). To see the intersections in detail, (*d*), (*e*) and (*f*) are zooms of (*a*), (*b*) and (*c*), respectively. The parameters used in every figure are $\beta_r=1.125$, $\beta_i=0.2298$, $\gamma_r=-0.859375$, $\gamma_i=D_i=0$ and $D_r=1$. Only μ is varied: (*a*) $\mu=-0.2340$, (*b*) $\mu=-0.2320$, (*c*) $\mu=-0.2290$.

The next step in the matching approach is to impose continuity on the functions at $x_c=-p/\alpha$. The continuity in $R_0(x)$ fixes the value of x_0 in terms of R_m and p,

$$x_0 = x_c + \frac{\ln u_*}{\sqrt{-\mu_+ + p^2}}, \tag{2.8}$$

where

$$u_*^2 = \frac{2\sqrt{b}}{r_c^2} - \frac{a}{\sqrt{b}} + \sqrt{\left(\frac{a}{\sqrt{b}} - \frac{2\sqrt{b}}{r_c^2}\right)^2 - \left(\frac{a^2}{b} - 4\right)} \tag{2.9}$$

and $r_c = R_m - \varepsilon x_c^2$.

The continuity of $R_{0x}(x)$ at $x=x_c$ gives us a relation between R_m and p,

$$f(R_m, p) \equiv \sqrt{-\frac{\gamma_+}{3}}\, r_c \sqrt{r_c^4 - a r_c^2 + b} + 2\varepsilon x_c = 0. \tag{2.10}$$

A second relation emerges from a condition of consistency (Thual & Fauve 1988), obtained by multiplying equation (2.4) by $R_0(x)$ and integrating in the

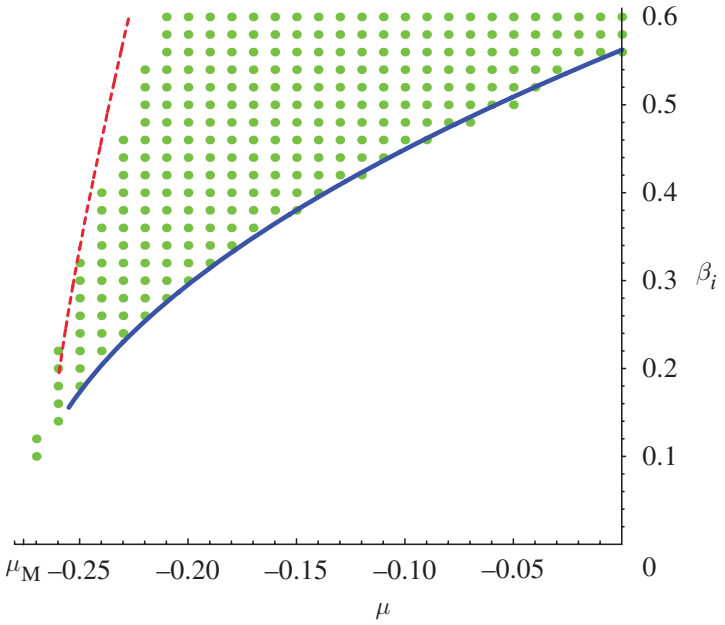

Figure 3. Pulses in the phase diagram (μ, β_i). Green dots are numerically simulated pulses. Blue solid line (on the right) is the curve associated with equation (3.6), which corresponds to the maximum value where pulses exist. Red dashed line (on the left) is the minimum value where pulses exist, and it is obtained from the matching approach. $\beta_r = 1.125$, $\gamma_r = -0.859375$, $\gamma_i = D_i = 0$, $D_r = 1$ and $\mu_M = -0.276136$.

real axis. Since $R_0(x)$ is a symmetric function, the relation is reduced to

$$g(R_m, p) \equiv \mu_- \int_{-\infty}^{0} R_0^2 \, dx - \beta_- \int_{-\infty}^{0} R_0^4 \, dx - \gamma_- \int_{-\infty}^{0} R_0^6 \, dx = 0. \tag{2.11}$$

The integrals can be evaluated as in Descalzi *et al.* (2002). The existence of pulses is restricted by the conditions $f(R_m, p) = 0$ and $g(R_m, p) = 0$ in the following way: pulses exist if the matching between the two regions (core and outside the core) takes place. This occurs when the conditions are simultaneously fulfilled, and graphically it implies the intersection between the curves defined in the (R_m, p) plane (figure 2).

Through this procedure, the mechanism of emergence of pulses has been explained: there is a critical value μ_{c1} at which, for $\mu < \mu_{c1}$, the curves $f = 0$ and $g = 0$ do not intersect, implying that there are no pulses. For $\mu > \mu_{c1}$, the curves intersect at two points that represent stable and unstable pulses. This means that the emergence mechanism of pulses is a saddle-node bifurcation (Descalzi *et al.* 2002, 2003).

3. Transition from pulses to fronts

(*a*) *Mathematical conditions*

As demonstrated in Gutiérrez & Descalzi (2007), from a mathematical point of view, the disappearance of pulses is related to R_0, which is assumed to be real. If μ is increased above the critical value μ_{c2}, R_0 is no longer real. For that reason,

pulses cannot exist. The region in the (R_m, p) plane, where R_0 does not exist as a real variable, will be called R (figure 2). When μ is increased, R invades the (R_m, p) space. If the intersection of the curves $f=0$ and $g=0$ (in blue and purple, respectively) takes place in R, the pulse does not exist. That is the case of figure 2*c* (zoom in figure 2*f*).

In conclusion, there is a qualitative change in the system at μ_{c2}, where pulses stop existing. At μ_{c2}, the intersection of $f=0$ and $g=0$ takes place at the border of R, which is a straight line defined by the condition $u_*^2=0$ (it implies $a^2=4b$, or $\left(-p^2+\mu_+\right)=3\beta_+^2/16\gamma_+$), which fixes p in the constant value p_c

$$p_c^2=\frac{D_r\mu-\alpha_1+\sqrt{\alpha_2-\alpha_3\mu}}{D_r^2}, \tag{3.1}$$

with

$$\alpha_1=\frac{3}{16}\frac{(D_r\beta_r+D_i\beta_i)^2}{D_r\gamma_r+D_i\gamma_i}\left(1+\frac{D_i^2}{|D|^2}\right), \qquad \alpha_2=\left(\frac{3D_i}{8|D|}\frac{(D_r\beta_r+D_i\beta_i)^2}{D_r\gamma_r+D_i\gamma_i}\right)^2$$

and

$$\alpha_3=\frac{3D_rD_i^2}{4|D|^2}\frac{(D_r\beta_r+D_i\beta_i)^2}{D_r\gamma_r+D_i\gamma_i}.$$

In the dispersion-less case of $D_i=0$ and $D_r=1$, coefficients α are reduced to $\alpha_1=3\beta_r^2/16\gamma_r\equiv\mu_M$ (μ of Maxwell), $\alpha_2=\alpha_3=0$, and expression (3.1) takes the simpler form

$$p_c^2=\mu-\mu_M. \tag{3.2}$$

To obtain μ_{c2}, we explicitly write $f(R_m,p,\mu)$ and $g(R_m,p,\mu)$, and then remove p taking into consideration that p_c depends only on μ, as can be seen in equation (3.1). In this case, when p tends to p_c, the expression of g takes the form (more details are given in Gutiérrez & Descalzi (2007))

$$g_{p\to p_c}(R_m,\mu)\equiv 8\mu_- -4\beta_- a-\gamma_-(3a^2-4b)=0. \tag{3.3}$$

The above expression depends only on μ. Then μ_{c2} can be obtained explicitly,

$$\mu_{c2}=\frac{\alpha_2-(\alpha_1-D_r\alpha_4)^2}{\alpha_3}, \tag{3.4}$$

where

$$\alpha_4=\frac{3}{4}\frac{D_r\beta_r+D_i\beta_i}{D_r\gamma_r+D_i\gamma_i}\left(\beta_r-\frac{3}{4}\gamma_r\frac{D_r\beta_r+D_i\beta_i}{D_r\gamma_r+D_i\gamma_i}\right).$$

If we take the dispersion-less limit $D_i=0$, using $D_r=1$ and defining $\alpha_5=(2\beta_i a+\gamma_i a^2)/8\sqrt{-\mu_M}$, we get a simpler expression of μ_{c2}, which is

$$\mu_{c2}=\mu_M+\alpha_5^2. \tag{3.5}$$

(*b*) *Analytical prediction and numerical simulations*

Equation (2.1) has seven parameters, but only four of them are relevant, because we can re-scale amplitude A, space x and time t. As a particular case, we can fix other parameters such as $\gamma_i=D_i=0$ and only two are necessary to

describe the system. We will use μ as before, because it is the control parameter. As the second parameter, we will use β_i because it is the only non-variational parameter ($D_r = 1$ for simplicity).

The phase diagram (μ, β_i) is not simple *a priori*. From a numerical study, it is possible to observe a lot of different localized solutions, as can be seen in Descalzi *et al.* (2005). In this case, our goal is simpler. It is to compare numerical simulations with the limit for the existence of pulses given by equation (3.5), which is obtained from the matching approach.

Rewriting the earlier mentioned equation, we obtain

$$\beta_i(\mu) = \frac{9\gamma_i\beta_r^2 - 32\gamma_r^2\sqrt{\mu_{\mathrm{M}}(\mu_{\mathrm{M}} - \mu)}}{12\gamma_r\beta_r}, \tag{3.6}$$

and can plot a curve in the space (μ, β_i), which can be seen as the blue solid line on the right in figure 3.

For numerical computations, we use RK4 with $\mathrm{d}t = 0.1$, $\mathrm{d}x = 0.4$ and 600 points to get a spatial box of $L = 240$. Localized structures are selected by the system, given the parameters and an initial condition. We use the initial condition *in phase* (Descalzi *et al.* 2005). In figure 3, the green dots correspond to numerically simulated pulses. At the transition to fronts, their existence boundary is in good agreement with the curve obtained from equation (3.6) (blue solid curve).

(*c*) *Width of pulses*

As can be seen from figure 4, if μ is increased near the critical value $\mu_{\mathrm{c}2}$, the width of pulses enlarges abruptly. Then, studying the width of pulses could be useful to characterize the transition from pulses to fronts, and it can be done using the matching approach. One possible way to define the width Δ is by measuring it at the half height of the pulse,

$$\Delta = 2|x_m|, \tag{3.7}$$

where x_m is the half width, defined to satisfy $R_0(x_m) = R_{\mathrm{m}}/2$. Then it is equal to

$$x_m = x_0 - \frac{\ln s_m}{\sqrt{-\mu_+ + p^2}}, \tag{3.8}$$

with

$$s_m^2 = \frac{8\sqrt{b}}{R_{\mathrm{m}}^2} - \frac{a}{\sqrt{b}} + \frac{8}{R_{\mathrm{m}}^2}\sqrt{\frac{R_{\mathrm{m}}^4}{16} - \frac{aR_{\mathrm{m}}^2}{4} + b}.$$

If we use expression (2.8) of x_0, we obtain another equation for the half width

$$x_m = x_{\mathrm{c}} + \frac{\ln(u^*/s_m)}{\sqrt{-\mu_+ + p^2}}, \tag{3.9}$$

which contains the same singularities of x_0 (since s_m does not reach zero in the whole range explored by us). In particular, when u^* tends to zero (at $\mu_{\mathrm{c}2}$), x_m diverges.

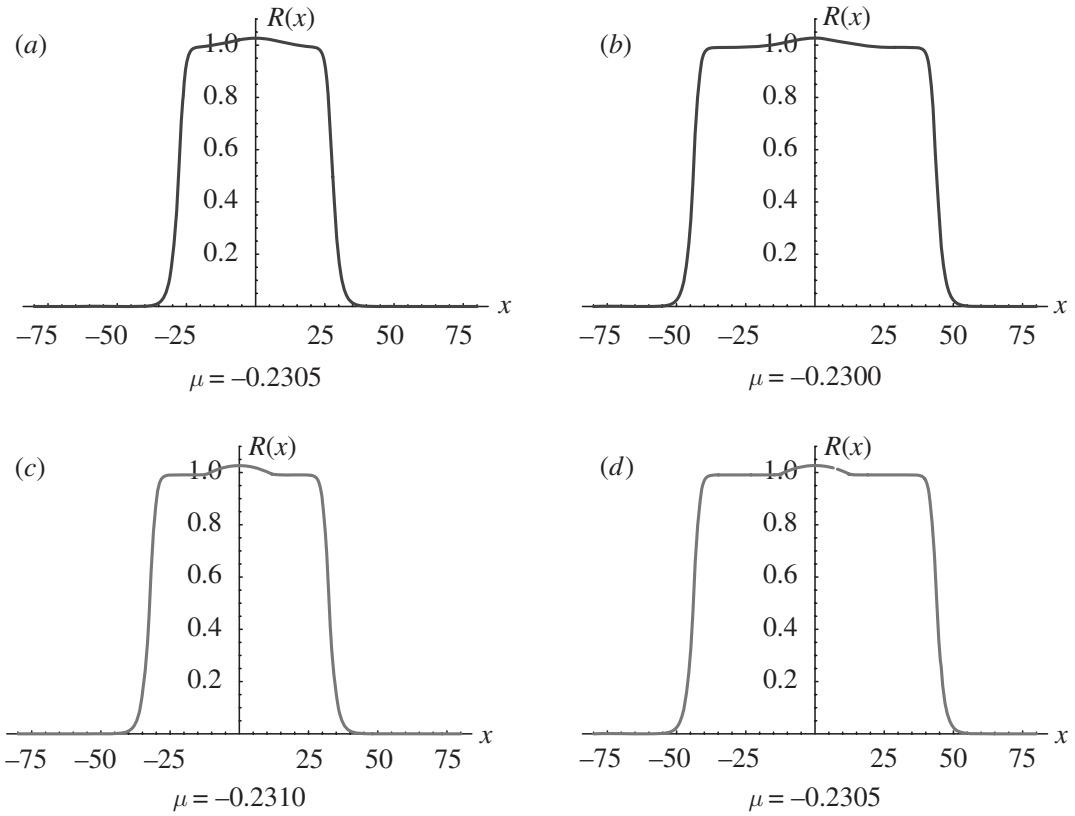

Figure 4. Pulses close to the transition to fronts. (*a*) and (*b*) are the result of direct numerical simulations of equation (2.1). In this case, at $\mu = -0.2299$, the system selects another solution and pulses cannot be observed. (*c*) and (*d*) are the approximated pulses done by the calculations presented in §2. Here, from equation (3.5), the expected value of transition is $\mu_{c2} = -0.230049$. Apart from μ, the parameters are the same as in figure 2.

Near μ_{c2}, the singularity of x_m shows that, in the transition to fronts, pulses become wider. This is presented in figure 5 (grey dashed line) and is compared with the numerical simulation (solid line). The width of pulses going to infinity is suggested in both computations. In the numerical case, infinite width cannot be observed since the numerical method (RK4) has finite resolution. Using $\mathrm{d}t = 0.1$ (our case), the parameters have a resolution of 10^{-4}.

In order to get bifurcation diagrams (figure 6), we add unstable pulses to the picture of stable pulses. Both exist since the bifurcation in the cubic–quintic CGL equation is sub-critical.

Considering both kinds of pulses, we re-obtain that their emergence takes place via saddle-node bifurcation (figure 6*b*). With regard to the disappearance of pulses, it can be said that the stable ones lead to fronts at μ_{c2} (increasing their width to infinity), and the width of unstable pulses also tends to infinity at $\mu = 0$, but its amplitude tends to zero, collapsing with the homogeneous state $A = 0$ (figure 6*c* and *d*).

Note that we are assuming that the stationary pulse obtained with the matching approach is stable for all $\mu \in [\mu_{c1}, \mu_{c2}]$. Our numerical study, keeping only the non-variational parameter β_i, is in good agreement with this assumption. However, it has been reported in a high dispersion case (Tsoy *et al.* 2006), where

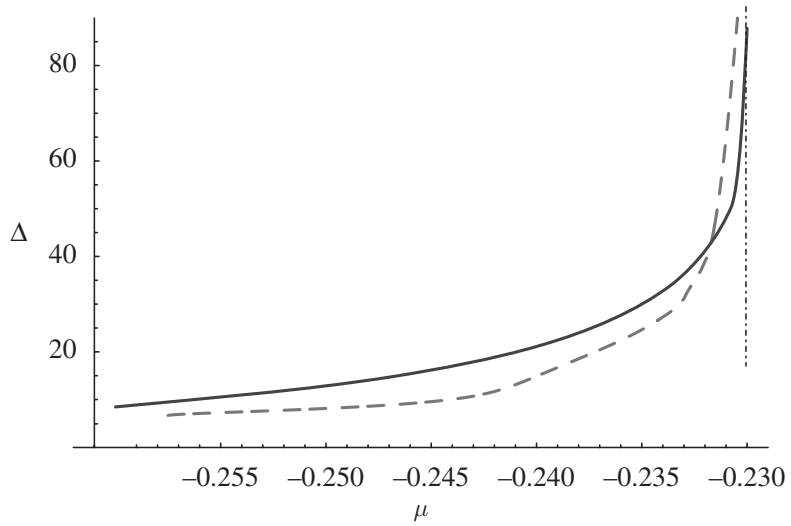

Figure 5. Width of stable pulses as a function of μ. The grey dashed line is the width calculated from equation (3.7). The solid line is the width measured from the numerically simulated pulses. The straight dotted line corresponds to $\mu_{c2} = -0.230049$, which is obtained from equation (3.5). Apart from μ, the parameters are the same as in figures 2 and 4.

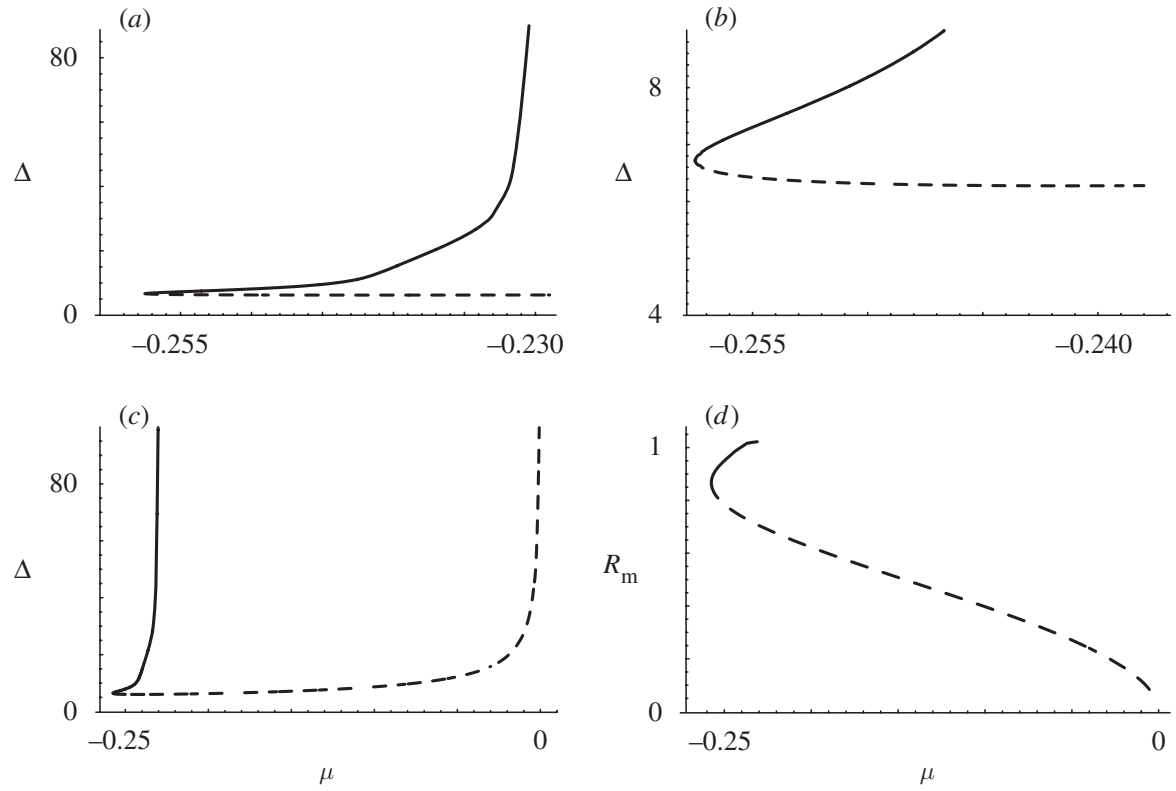

Figure 6. (a–c) Different views of the bifurcation diagram. It has been done from the approximating scheme. Solid line corresponds to stable pulses, and dashed line corresponds to unstable pulses. (a) Divergence of stable pulse when μ is close to μ_{c2}. (b) Emergence of pulses via saddle-node bifurcation. (c) Divergence of the width of both stable and unstable pulses, in a larger scale of μ. In (d), the maximum amplitude R_m for both kinds of pulses is shown. Note that R_m has no singularities (stable pulses exist in a smaller range of μ). Apart from μ, the parameters are the same as in figure 2.

pulses have a region of pulsating behaviours. Eventually, the stationary pulse undergoes a Andronov–Hopf bifurcation before the transition to front. This type of instability could give rise to more complex bifurcation diagrams (Chang *et al.* 2007), including chaotic behaviours.

(*d*) *Geometrical picture*

The bifurcation scenario that we are proposing for the transition from stationary pulses to fronts can be depicted in a more geometrical fashion. Actually, we can rewrite equations (2.3) and (2.4) as a three-dimensional dynamical system

$$R_{0x} = W, \tag{3.10}$$

$$W_x = -\mu_+ R_0 - \beta_+ R_0^3 - \gamma_+ R_0^5 + R_0 S^2, \tag{3.11}$$

$$S_x = \mu_- - \beta_- R_0^2 - \gamma_- R_0^4 - \frac{2WS}{R_0}, \tag{3.12}$$

where $S = \theta_{0x}$. Then, the stationary pulses that we analysed using the matching approach corresponds to a heteroclinic orbit of the earlier dynamical system, which links the hyperbolic points $(R_0, W, S) = (0, 0, p)$ and $(R_0, W, S) = (0, 0, -p)$. The value of p is obtained by the matching procedure.

Therefore, the stationary pulses are like a 'particle' that follows a trajectory (the heteroclinic orbit) in the phase space (R_0, W, S) of the dynamical system (3.10), (3.11) and (3.12), as the 'time' x runs. As μ increases and approaches the critical value μ_{c2}, the particle spends more time near the point $(R_0(x_c), R_{0x}(x_c), p)$, after it leaves the hyperbolic points $(0, 0, p)$ (i.e. outside the core). Then, it soundly changes from p to $-p$ (inside the core) and repeats the same pattern for $-p$, until it converges to the hyperbolic point $(0, 0, -p)$. In the limit $\mu \to \mu_{c2}^-$, the time spent near the points $(R_0(x_c), R_{0x}(x_c), \pm p)$ tends to infinity.

At the point $\mu = \mu_{c2}$, the dynamical system (3.10), (3.11) and (3.12) has a heteroclinic orbit that links the hyperbolic points $(0, 0, p_c)$ and $(\rho(\infty), 0, p_c)$ (as well as for $-p_c$), where

$$\rho(\infty) = \sqrt{\frac{-\beta_+ + \sqrt{\beta_+^2 - 4\left(\mu_+ - p_c^2\right)\gamma_+}}{2\gamma_+}}; \tag{3.13}$$

for that reason $(\mu_+ - p_c^2) = 3\beta_+^2/16\gamma_+$, which corresponds to the Maxwell point of equation (2.3) for a fixed $S \equiv p_c$. However, this orbit cannot be obtained from a pulse generated for $\mu < \mu_{c2}$. Moreover, it cannot be obtained numerically, because it demands an infinite size system. If the system has a finite size, we always need a source of waves, which is in fact the core of the pulse.

What we observe numerically is that the width of the pulse tends to infinity when μ increases and approaches the critical value μ_{c2}. For $\mu > \mu_{c2}$, we only observe a propagative behaviour, which is not achievable by equations (2.3) and (2.4) or equations (3.10)–(3.12), which are restricted for static solutions.

4. Conclusions

We were concerned with systems that are modelled by the cubic–quintic CGL equation. This equation accepts different stable solutions such as fronts and localized structures (pulses and holes). We studied analytically the transition from pulses to fronts.

More specifically, we reviewed an approximation scheme for pulses that give us mathematical conditions for their existence in the parameter space. Using that scheme, we obtained an analytical expression associated with the disappearance of pulses. In a particular case, we checked the analytical expression with numerical simulations by doing a phase diagram, and they are in good agreement.

In order to see what happens beyond pulses, we explored their width and saw that it diverges at the expected critical value. The divergence in the width was observed in numerical simulations too. Then, we concluded that pulses disappear giving rise to fronts. Because the width is a good variable to describe pulses, we constructed bifurcation diagrams. One of them, related to pulse emergence, is consistent with a previously known result.

It is important to emphasize that the scenario proposed in this paper is related to the stability of the stationary pulse, which is what is observed in most of the dispersion-less cases. In high-dispersion cases, a more complicated scenario is expected (Chang *et al.* 2007).

Finally, we conclude that with a simple approximation scheme for pulses, the matching approach, we can get important features of their dynamics.

The authors wish to acknowledge the support of FAI (Project ICIV-003-08, Universidad de los Andes, 2008), FONDECYT (Project No. 1070098), FONDECYT (Project No. 3070013) and Project Anillo en Ciencia y Tecnologia ACT15. The numerical simulations were done using the software DIMX, developed in the Institut Non Linéaire de Nice, France. The authors also thank Jaime Cisternas for helpful discussions.

References

Afanasjev, V. V., Akhmediev, N. & Soto-Crespo, J. M. 1996 Three forms of localized solutions of the quintic complex Ginzburg–Landau equation. *Phys. Rev. E* **53**, 1931–1939. (doi:10.1103/PhysRevE.53.1931)

Chang, W., Ankiewicz, A., Akhmediev, N. & Soto-Crespo, J. M. 2007 Creeping solitons in dissipative systems and their bifurcations. *Phys. Rev. E* **76**, 016 607-1–016 607-8. (doi:10.1103/PhysRevE.76.016607)

Deissler, R. J. & Brand, H. R. 1994 Periodic, quasiperiodic, and chaotic localized solutions of the quintic complex Ginzburg–Landau equation. *Phys. Rev. Lett.* **72**, 478–481. (doi:10.1103/PhysRevLett.72.478)

Descalzi, O. 2003 On the stability of localized structures in the complex Ginzburg–Landau equation. *Physica A* **327**, 23–28. (doi:10.1016/S0378-4371(03)00432-1)

Descalzi, O. & Brand, H. R. 2005 Stable stationary and breathing holes at the onset of a weakly inverted instability. *Phys. Rev. E* **72**, 055 202-1–055 202-4(R). (doi:10.1103/PhysRevE.72.055202)

Descalzi, O., Martinez, S. & Tirapegui, E. 2001 Thermodynamic potentials for non-equilibrium systems. *Chaos Solitons Fractals* **12**, 2619–2630. (doi:10.1016/S0960-0779(01)00077-7)

Descalzi, O., Argentina, M. & Tirapegui, E. 2002 Stationary localized solutions in the subcritical complex Ginzburg–Landau equation. *Int. J. Bifur. Chaos* **12**, 2459–2465. (doi:10.1142/S0218127402005960)

Descalzi, O., Argentina, M. & Tirapegui, E. 2003 Saddle-node bifurcation: appearance mechanism of pulses in the subcritical complex Ginzburg-Landau equation. *Phys. Rev. E* **67**, 015 601-1–015 601-4(R). (doi:10.1103/PhysRevE.67.015601)

Descalzi, O., Gutiérrez, P. & Tirapegui, E. 2005 Localized structures in nonequilibrium systems. *Int. J. Mod. Phys. C* **16**, 1909–1916. (doi:10.1142/S0129183105008424)

Descalzi, O., Brand, H. R. & Cisternas, J. 2006*a* Hysteretic behavior of stable solutions at the onset of a weakly inverted instability. *Physica A* **371**, 41–45. (doi:10.1016/j.physa.2006.04.085)

Descalzi, O., Cisternas, J. & Brand, H. R. 2006*b* Collisions of pulses can lead to holes via front interaction in the cubic–quintic complex Ginzburg–Landau equation in an annular geometry. *Phys. Rev. E* **74**, 065 201-1–065 201-4(R). (doi:10.1103/PhysRevE.74.065201)

Descalzi, O., Cisternas, J., Gutiérrez, P. & Brand, H. R. 2007 Collisions of counter-propagating pulses in coupled complex cubic–quintic Ginzburg–Landau equations. *Eur. Phys. J. Spec. Top.* **146**, 63–70. (doi:10.1140/epjst/e2007-00169-8)

Fauve, S. & Thual, O. 1990 Solitary waves generated by subcritical instabilities in dissipative systems. *Phys. Rev. Lett.* **64**, 282–284. (doi:10.1103/PhysRevLett.64.282)

Gutiérrez, P. & Descalzi, O. 2007 Existence range of pulses in the quintic complex Ginzburg–Landau equation. In *Nonequilibrium statistical mechanics and nonlinear physics* (eds O. Descalzi, O. A. Rosso & H. A. Larrondo), pp. 127–132, *AIP Conf. Proc.*, no. 913. Melville, NY: American Institute of Physics.

Hakim, V. & Pomeau, Y. 1991 On stable localized structures and subcritical instabilities. *Eur. J. Mech. B/Fluids* **10**, 137–143.

Hayase, Y., Descalzi, O. & Brand, H. 2004 Coexistence of stable particle and hole solutions for fixed parameter values in a simple reaction diffusion system *Phys. Rev. E* **69**, 065 201-1–065 201-4(R). (doi:10.1103/PhysRevE.69.065201)

Kolodner, P. 1991 Collisions between pulses of traveling-wave convection. *Phys. Rev. A* **44**, 6466–6479. (doi:10.1103/PhysRevA.44.6466)

Kolodner, P., Bensimon, D. & Surko, C. M. 1988 Traveling-wave convection in an annulus. *Phys. Rev. Lett.* **60**, 1723–1726. (doi:10.1103/PhysRevLett.60.1723)

Malomed, B. A. & Nepomnyashchy, A. A. 1990 Kinks and solitons in the generalized Ginzburg–Landau equation. *Phys. Rev. A* **42**, 6009–6014. (doi:10.1103/PhysRevA.42.6009)

Sakaguchi, H. 1991 Hole Solutions in the complex Ginzburg–Landau equation near a subcritical bifurcation. *Prog. Theor. Phys.* **86**, 7–12. (doi:10.1143/PTP.86.7)

Thual, O. & Fauve, S. 1988 Localized structures generated by subcritical instabilities. *J. Phys. France* **49**, 1829–1833. (doi:10.1051/jphys:0198800490110182900)

Tsoy E., Ankiewicz A. & Akhmediev N. 2006 Dynamical models for dissipative localized waves of the complex Ginzburg–Landau equation. *Phys. Rev. E* **73**, 036 621-1–036 621-10. (doi:10.1103/PhysRevE.73.036621)

van Saarloos, W. & Hohenberg, P. C. 1990 Pulses and fronts in the complex Ginzburg–Landau equation near a subcritical bifurcation. *Phys. Rev. Lett.* **64**, 749–752. (doi:10.1103/PhysRevLett.64.749)

van Saarloos, W. & Hohenberg, P. C. 1992 Fronts, pulses, sources and sinks in generalized complex Ginzburg–Landau equations. *Physica D* **56**, 303–367. (doi:10.1016/0167-2789(92)90175-M)